Chemical Engineering Communications

Publication details, including instructions for authors and subscription information:
http://www.informaworld.com/smpp/title~content=t713454788

DIRECT CONTACT CONDENSATION OF DILUTE STEAM/AIR MIXTURES ON WAVY FALLING FILMS

T. D. Karapantsios [a]; M. Kostoglou [a]; A. J. Karabelas [a]
[a] Department of Chemical Engineering, Chemical Process Engineering Research Institute and, Aristotle University of Thessaloniki Univ, Thessaloniki, GR, Greece

Online Publication Date: 01 November 1994
To cite this Article: Karapantsios, T. D., Kostoglou, M. and Karabelas, A. J. (1994) 'DIRECT CONTACT CONDENSATION OF DILUTE STEAM/AIR MIXTURES ON WAVY FALLING FILMS', Chemical Engineering Communications, 141:1, 261 - 285
To link to this article: DOI: 10.1080/00986449608936419
URL: http://dx.doi.org/10.1080/00986449608936419

Chem. Eng. Comm., 1996, Vols. 141–142, pp. 261–285
Reprints available directly from the publisher
Photocopying permitted by license only

DIRECT CONTACT CONDENSATION OF DILUTE STEAM/AIR MIXTURES ON WAVY FALLING FILMS

T. D. KARAPANTSIOS, M. KOSTOGLOU and A. J. KARABELAS

Chemical Process Engineering Research Institute and
Department of Chemical Engineering, Aristotle University of Thessaloniki
Univ. Box 455, GR 540 06 Thessaloniki, Greece

(Received in final form April 24, 1995)

Condensation from air-steam mixtures on falling water layers is investigated experimentally and theoretically. The thin film flows on the inner surface of a 5 cm i.d. vertical pipe. This film is wavy turbulent while the gas phase is kept saturated with steam. Experiments are conducted with the gas mixture effectively stagnant, compared with the fast moving liquid film. Measurements are also made under a mild vacuum applied on the gas phase. Heat transfer coefficients averaged over the entire length of the condensing surface, tend to increase by decreasing the liquid flowrate, by increasing the steam fraction, and by applying a mild vacuum on the gas phase. However, for the cases examined, there is a liquid flowrate above which the heat transfer coefficient becomes almost constant.

Numerical predictions are made for a fully developed turbulent film using an eddy diffusivity model. The results indicate that for a system with a large amount of noncondensable gases–as in this study–the temperature profile in the liquid film is nearly uniform and that the major resistance to condensation resides in the gas phase. The analysis also shows that the relative contribution of sensible heat transferred through the gas phase is small relative to the latent heat released upon condensation. Comparison of predictions with experimental data suggests that a significant parameter in these analyses is the gas diffusion boundary layer thickness which seems to be comparable in size with the liquid film thickness. Finally, the possibility is discussed of correlating condensation heat transfer coefficients with already available statistical characteristics of the falling wavy layer. Theoretical predictions based on this idea are in good agreement with data.

KEYWORDS Direct contact condensation Noncondensables Steam/air Falling films

INTRODUCTION

Attention has been focused in recent years on direct contact condensers where the vapor is condensed directly on moving layers or droplets of subcooled liquid. Interest has been generated by water desalination equipment design and by energy conversion applications, such as geothermal, solar and nuclear energy systems (Kreith and Boehm, 1988). Among the main advantages of these condensers one can include their simple design, minor fouling problems and high specific transfer areas and rates. Thus they represent a very tempting option since their ability to condense a specified amount of vapor is dictated (and limited) only by the energy balance between latent heat of condensation and the sensible heat that can be absorbed by the subcooled liquid.

A survey of contributions on this topic has been recently published by Jacobs (1988). Serious gaps are identified in the literature concerning both basic understanding of the

process (especially when noncondensable gases are present) and availability of reliable design procedures.

The present study is concerned with direct contact condensers in which falling thin liquid layers are flowing on solid substrates, e.g. packing or pipe surface. Relevant work in the literature refers mostly to *pure vapor* condensation on the same liquid compound or other immiscible liquid, for either the case of a flat vertical plate (e.g. Jacobs, 1980; Rao and Sarma, 1984) or a nearly vertical rectangular channel (e.g. Kim *et al.*, 1985). Significant work by Bankoff and co-workers (1983, 1985) and Celata and co-workers (1989, 1991) involves pure vapor condensation in horizontal and inclined channels, while Tamir and co-workers (1974, 1976) treat the case of thin falling films of spherical geometry. However, the effects associated with the presence of noncondensables are not adequately dealt with, while most studies assume laminar film flow, free of turbulence and waviness. To the best of the authors' knowledge, direct-contact condensation on wavy turbulent falling films with noncondensables present (studied here) is not addressed at all in the literature despite its practical significance.

This work is motivated by a parallel project carried out in this Laboratory (Bontozoglou and Karabelas, 1993) for the separation of noncondensable gases from high pressure geothermal steam by means of a column filled with structured packing, operating as a direct contact device for the subcooled water and the geothermal gaseous stream. The function of this column is to disengage the noncondensable H_2S and CO_2, before steam utilization in turbines, by condensing the water vapor under high pressure. As Fair and Bravo (1990) state, mass transfer data for round wetted-wall columns agree fairly well with experimental results from structured packings, indicating that the corrugated surface of the latter is essentially completely wetted. Thus the relatively simple falling film geometry is considered appropriate for studying the problem at hand.

One of the main issues addressed here is the effect of *large amounts of noncondensables* which appear to be responsible for dramatic alterations of the transfer rates. Most previous work (e.g. Minkowycz and Sparrow, 1966) deals with relatively small amounts of noncondensables ($\leqslant 10\%$ mass fraction), although a relatively recent paper reports data taken with large air/steam ratios (Barry and Corradini, 1988). Yet, the latter tests are conducted in a horizontal stratified two-phase flow geometry. Furthermore, the effect of interfacial waves on the transfer process has received little attention, and only for the case of relatively thick liquid layers (greater than ~ 2 mm), moving horizontally (Barry, 1987). Thus another objective of this work is to collect data helpful in shedding some light on liquid/vapor *interface wave effects.*

The experiments reported here are carried out in a vertical test section, long enough so that practically fully developed flow conditions are attained by the falling liquid. The hydrodynamics of such free falling films have already been investigated in this Laboratory (Karapantsios *et al.*, 1989; Karapantsios and Karabelas, 1990). The new results involve heat transfer and condensation rates *averaged* over the entire length of the condensing (inner pipe) surface. Care is taken in the tests to minimize convective currents of the air-steam mixture in the pipe core, in order to render that mixture effectively stagnant by comparison with the (downward) fast moving liquid film. Thus, considering that no significant shear is exerted on the interface from the gaseous phase, an attempt is made to isolate the role played by the interfacial waves on the transport

process. It is of particular interest to explore the effect of such waves in the case of gas mixtures rich in noncondensables, since then the resistance to heat transfer very likely resides in the *gas* phase. Another motivation for reducing convective currents in the mixture is to approximate conditions prevailing in the aforementioned (Bontozoglou and Karabelas, 1993) direct contact condensation column. Indeed, as steam condensation proceeds along that column, the mixture is depleted of steam and the gas stream velocity is greatly reduced, becoming very small compared with liquid film velocity.

It is common practice in this type of equipment to apply a mild vacuum in order to facilitate removal of noncondensables and to improve overall column performance. Thus, the influence of a *mild vacuum* on condensation is also explored in this study by determining average condensation coefficients. Such information is not available in the literature for vertical condensers.

In the next section certain key simplifications in the theoretical problem formulation are assessed, leading to the development of a realistic, yet sufficiently simple, model which is used for predictions and data interpretation. The experimental set-up is outlined and the results are summarized next. Finally, the possibility is examined of correlating condensation heat transfer rates with already available statistical properties of the falling wavy layer.

THEORY

The presence of noncondensables in the gas phase causes remarkable reductions in condensation heat transfer rates. This is because the vapor has to diffuse through a layer of noncondensable compounds to reach the subcooled liquid film. The gas layer evidently acts as an additional resistance to heat transfer as indicated in Figure 1. In the present problem formulation, energy conservation in the moving liquid layer is employed. Free or forced convection in the gas phase are not taken into account

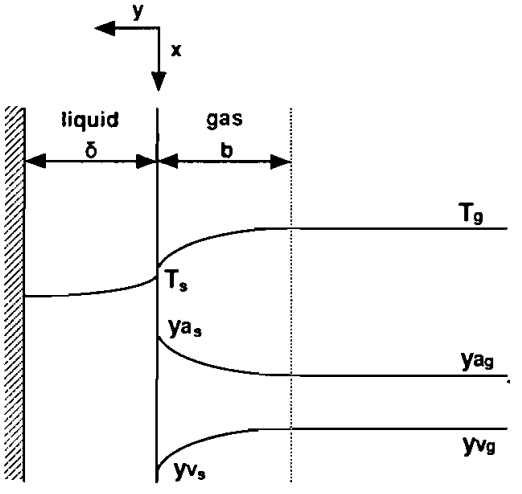

FIGURE 1 Interface resistance to heat transfer due to the presence of noncondensable gases.

explicitly, but instead a phenomenological description is used. However, the extent to which convection affects the transport process is a matter of concern, to be dealt with in a subsequent study.

The system of coordinates as well as notation employed here are shown in Figure 1. Neglecting motion in the lateral direction, the energy equation describing the thermal field inside the liquid layer can be written as

$$u(y)\frac{\partial T}{\partial x}=\frac{\partial}{\partial y}\alpha_e(y,T)\frac{\partial T}{\partial y} \tag{1}$$

where $u(y)$ is the streamwise velocity of the liquid film defined as

$$u(y)=\frac{u^{*2}}{\nu}\int_0^{\delta-y}\frac{1-\frac{y}{\delta}}{1+\frac{\varepsilon}{\nu}(y)}dy \tag{2}$$

where u^* is the friction velocity, $u^*=(g\delta)^{1/2}$, and $\alpha_e(y,T)$ is the effective thermal diffusivity taken as the sum of molecular and eddy diffusivity, i.e.

$$\alpha_e(y,T)=\alpha(T)+\frac{\varepsilon}{\nu}(y)\frac{\nu(T)}{Pr_T(y)} \tag{3}$$

Here the turbulent Prandtl number Pr_T is obtained from a correlation of data by Ueda *et al.* (1977), which is claimed to satisfactorily represent the turbulence structure near the interface:

$$Pr_T=1.4\exp\left(-15\frac{y}{\delta}\right)+0.66 \tag{4}$$

For the eddy viscosity $\varepsilon/\nu(y)$, an expression proposed by Mudawar and El-Masri (1986) is selected. Thus, given the liquid mass flow rate per unit circumferential length Γ, the film thickness δ is obtained by solving the equation

$$\frac{\Gamma}{\rho\delta}=\frac{u^{*2}}{\nu}\int_0^{\delta}\int_0^{y}\frac{1-\frac{x}{\delta}}{1+\frac{\varepsilon}{\nu}(x)}dxdy \tag{5}$$

The success of this approach in correlating mean film thickness data from our experimental setup (Karapantsios *et al.*, 1989) is shown in Figure 2.

The boundary conditions representative of our system are

$$x=0,\quad T=T_i \tag{6}$$

$$y=0,\quad -k\frac{dT}{dy}=q(T) \tag{7}$$

$$y=\delta,\quad -k\frac{dT}{dy}=0 \tag{8}$$

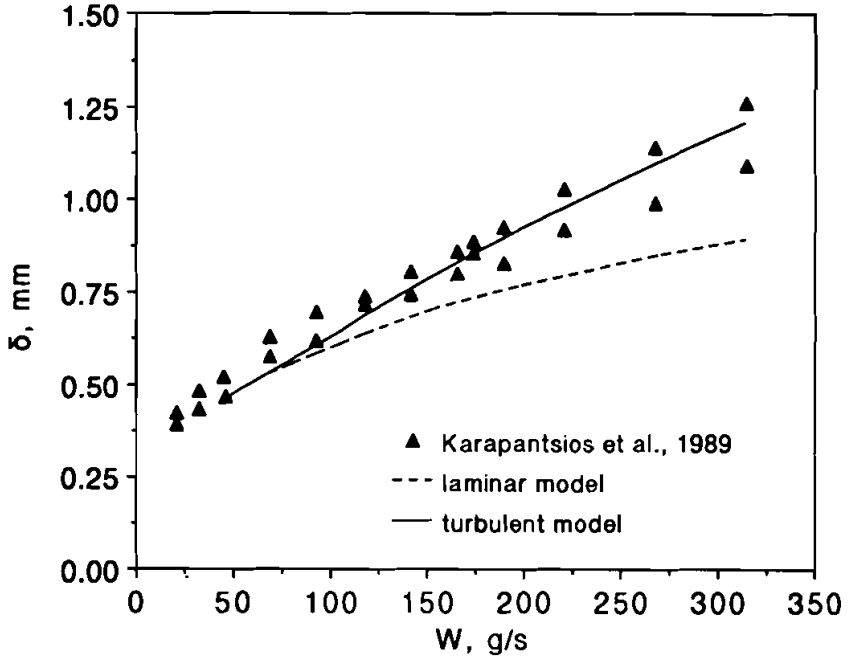

FIGURE 2 Liquid film thickness versus inlet liquid flow rate. Predictions by Nusselt, 1916 (laminar model). Predictions by Mudawar and El-Masri, 1986 (turbulent model).

where k is the liquid thermal conductivity. Adiabatic conditions (B.C. [8]) are considered to represent this system well.

The resistance to heat transfer on the gas side is considered next. Owing to accumulation of noncondensable gases near the interface, the condensing vapor must diffuse through a gas layer to reach the subcooled liquid film (Fig. 1). This diffusion gives rise to concentration and temperature gradients in the y-direction which are associated with a finite diffusive flux towards the interface. The heat transfer rate from the bulk gas mixture to the interface—at a point x along the pipe and for fixed total pressure, gas concentration and flow pattern—is given by (e.g. Collier, 1972)

$$q(T) = \frac{K_g \lambda \rho_g}{p_{\text{am}}}(p_{vg} - p_{vs}) + h_g(T_g - T_S) \tag{9}$$

where

$K_g = D_g/b$ is the mass transfer coefficient,

$h_g = k_g/b'$ is the sensible heat transfer coefficient,

$p_{\text{am}} = (p_{as} - p_{ag})/\ln(p_{as}/p_{ag})$ is the log mean partial pressure of noncondensable gas between the interface and the bulk (a = noncondensable gas, v = vapour, g = bulk gas mixture, s = surface).

The other variables define usual physical properties. It is noted that two length parameters (b and b') are introduced in the definitions of K_g and h_g. These are usually referred to as the *apparent mass* and *thermal boundary layers* at the gas side. It will be shown that the second term on the R.H.S. of [9] has a relatively small contribution to the overall heat transfer rate. Thus, one can take $b = b'$ without committing a significant error.

The above expression for the heat transfer on the gas side is strictly applicable at a fixed location along the test pipe. This is so, because the boundary layer value b is expected to vary with x in real situations, even if the gas phase bulk velocity is small or constant. In fact, b is affected by the details of the *gas* phase flow pattern near the interface where the liquid surface waves play a major role. These flow pattern details are impossible to describe at present. Therefore, for the purpose of this investigation, it is considered fruitful to utilize an average boundary layer value over the entire test section in correlating our integral condensation data. This simplification, despite its obvious shortcomings, allows one to interpret the data and relate them to film characteristics.

Integration of (1) with respect to y and division by δ, together with (7) and (8), gives

$$\frac{dT_{ave}}{dx} = \frac{1}{U_{ave}\delta\rho c_p} q(T_{y=0}) \tag{10}$$

where T_{ave} is the mass flow weighted average temperature across the film, defined as

$$T_{ave} = \frac{\int_0^\delta Tu\,dy}{\int_0^\delta u\,dy} \tag{11}$$

and U_{ave} is the average streamwise velocity defined as

$$U_{ave} = \frac{1}{\delta}\int_0^\delta u\,dy \tag{12}$$

For a flat temperature profile, $T_{ave} \cong T_{y=0} \cong T$, and (10) reduces to the simple form:

$$\frac{dT}{dx} = \frac{1}{U_{ave}\delta\rho c_p} q(T) \tag{13}$$

which corresponds to a negligible resistance to heat transfer within the liquid film. This implies that the film is capable of absorbing instantaneously all the heat released by condensation at the interface. The computational convenience associated with (13) is evident. However, the validity and significance of such a simplification needs to be assessed. Analytical solutions presented in the Appendix permit a quick assessment of the validity of the constant liquid temperature profile for various sets of parameters. Moreover, a rigorous numerical procedure is implemented to solve (and compare results from) (1) and (13) with B.C.'s (6), (7), (8) as outlined below.

In subsequent calculations, the variation of liquid properties within the flowing film is taken into account at each point of the computational grid, while for the gas phase all physical properties are evaluated at the bulk temperature of the mixture. All property values are obtained from VDI-Wärmeatlas (1974). It appears that the reliability of

computational results is significantly affected by the proper choice of fluid properties, as also reported by Minkowycz and Sparrow (1966).

A semi-implicit third order Runge-Kutta routine is used to obtain a solution of the system of Equations (1) through (9), henceforth to be referred to as "exact" solution. Cubic-spline polynomials are used to represent the temperature in the y-direction, permitting a fairly good approximation of the temperature gradient at the gas/liquid interface. An "approximate" solution is also obtained easily using a flat temperature profile, (13). Results for a low initial liquid flow rate ($W = 42.1$ g/s) are compared in Figure 3 (air mole fraction 0.85; $b = 1.5$ mm). In these calculations, the thickness b is evaluated by matching the computed film outlet temperature T_0 with the measured one for the case of a flat liquid T-profile and then this b value is used in the exact solution, too. Figure 3 reveals that the agreement of the two solutions is satisfactory, considering the fact that the flow rate is the most unfavorable encountered in this study. Indeed, for larger flow rates the increased thermal diffusivity–due to the increasing contribution of the turbulent eddy diffusivity–would tend to eliminate any thermal gradients within the liquid layer, leading to a better agreement of the two approaches. It will be noted that the effective thermal diffusivity may be up to 50 times greater than the molecular diffusivity for the larger liquid flow rates of this study.

To assess the main assumption involved in the development of (13), computed representative temperature profiles are displayed in Figure 4. They correspond to the conditions of Figure 3 which is the worst case for (1) to be tailored to fit (13). The temperature is plotted in the form of $\Delta T = (T_O - T_i)$ values, scaled as indicated in the

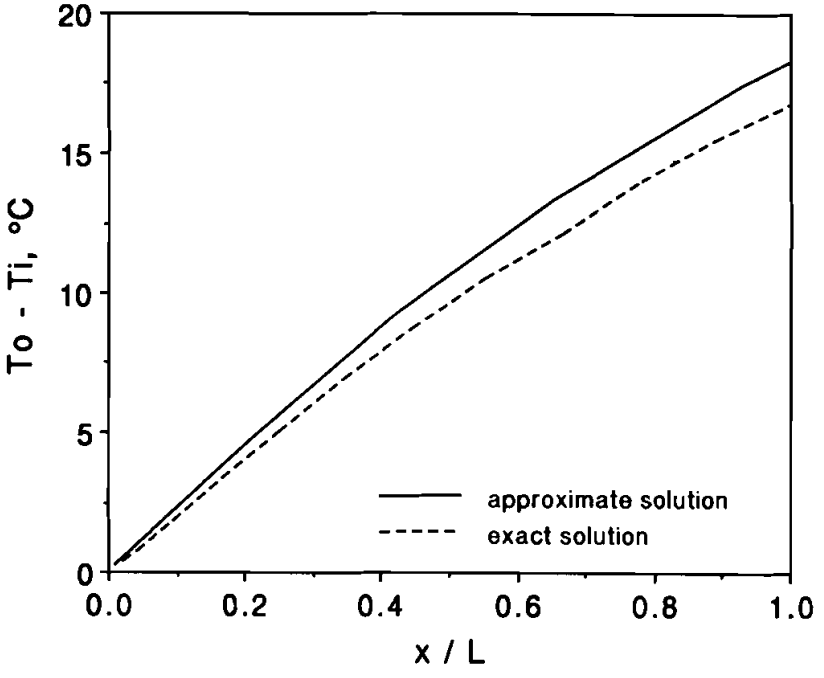

FIGURE 3 Comparison between the exact and approximate solution of the model equations. $W = 42.1$ g/s.

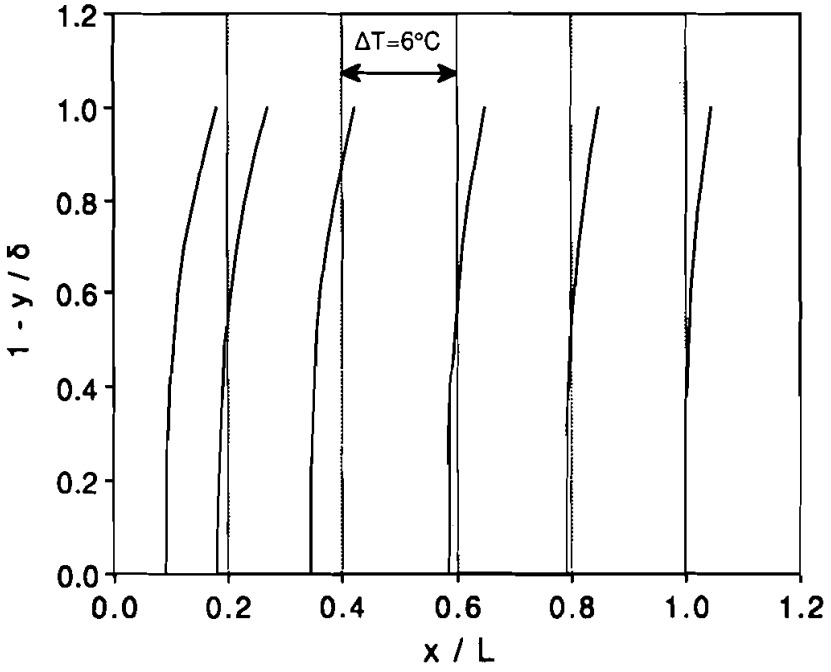

FIGURE 4 Temperature profiles across the liquid film for $W = 42.1$ g/s along the condensing surface.

graph. In this figure, $1 - y/\delta = 0$ represents the wall and $1 - y/\delta = 1$ represents the interface. At first glance, it appears that there is a small temperature change between the interface and the wall, especially for locations $x/L < 0.5$. However, this change is not considered significant for the determination of the average temperature across the film, since over most of the film cross section, $(1 - y/\delta < 0.5)$, $T_O - T_i$ is practically constant. The flat temperature approximation is quite accurate at large downstream distances and at high liquid flow rates.

Therefore, the "approximate" method is recommended as it combines satisfactory accuracy and insignificant computational labour. This method is used in the calculations and comparisons that follow. It will be noted that the same results can be obtained by assuming a flat velocity profile for the liquid film and employing the analytical solutions presented in the Appendix.

Some insight into the significant role played by the noncondensables can be gained by plotting (Fig. 5) the interfacial temperature T_S with respect to x/L, at various air mole fractions. The conditions ($W = 42.1$ g/s) are the same as those of Figure 3. In all cases, saturation is assumed for the gas phase. The axial temperature profiles for the largest air fractions are almost linear, indicating that greater (longer) condensing surface is needed to achieve high heat removal, in contrast to the smaller fractions where just about half of the available length is required.

Figure 6 shows on a percentage basis the relative contribution of the sensible heat, transferred through the diffusion layer, to the overall heat transferred. The function $q(T)$ is defined in (9). In this figure, ΔT depicts the difference $T_g - T_S$. The results show

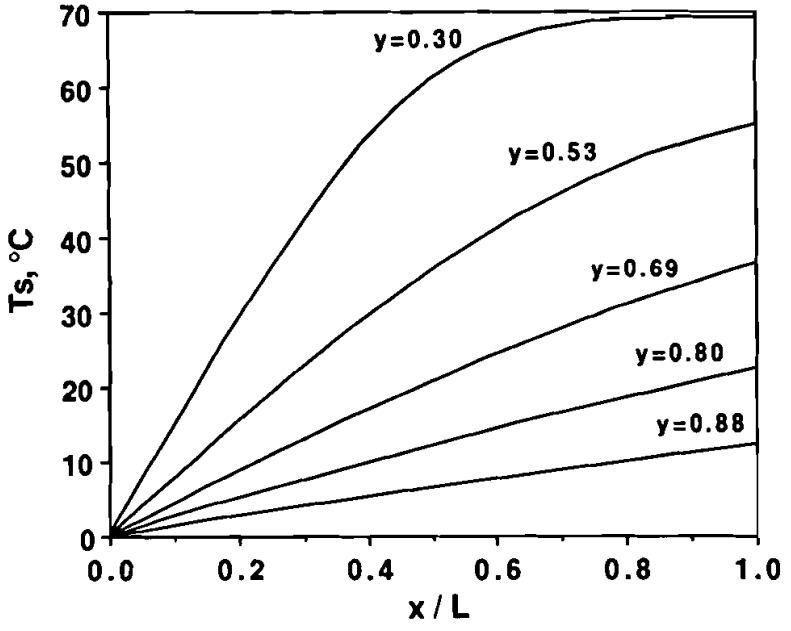

FIGURE 5 Axial variation of liquid surface temperature, at various fractions y of noncondensables.

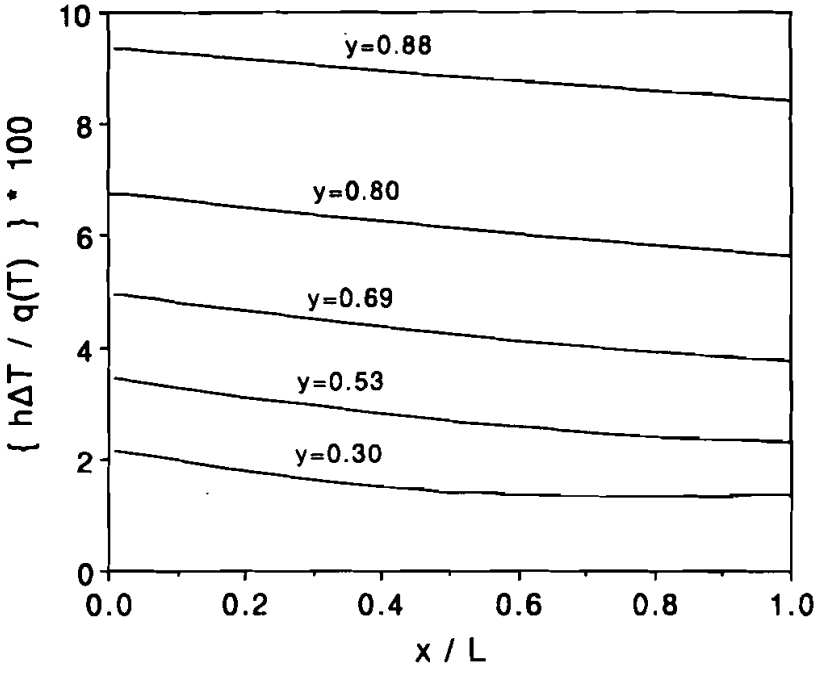

FIGURE 6 Contribution of sensible heat transfer ($h\Delta T$) to the overall heat transfer at relatively large noncondensable gas fractions.

that, while sensible heat transfer is very nearly negligible in the case of pure vapors or even vapors with a small amount of inert gases, it may become an appreciable factor ($\sim 10\%$) during condensation of vapors that contain large quantities of noncondensable gases. Of course, 10% is still a relatively small contribution, in which case the assumption to take the mass boundary layer as equal to the thermal one is reasonable.

APPARATUS AND EXPERIMENTS

The experimental setup is shown in Figure 7. The basic features of this system are similar to those reported by Karapantsios *et al.* (1989), with some major improvements. A vertical, transparent, plexiglas pipe of 50 mm ID and 2.66 m total length is used, divided in three sections, i.e. inlet (0.3 m), intermediate (0.96 m) and measurement section (1.40 m). The latter is equipped with six pairs of (diametrically opposite) thermocouples, mounted in special plugs, almost flush with the inner surface of the

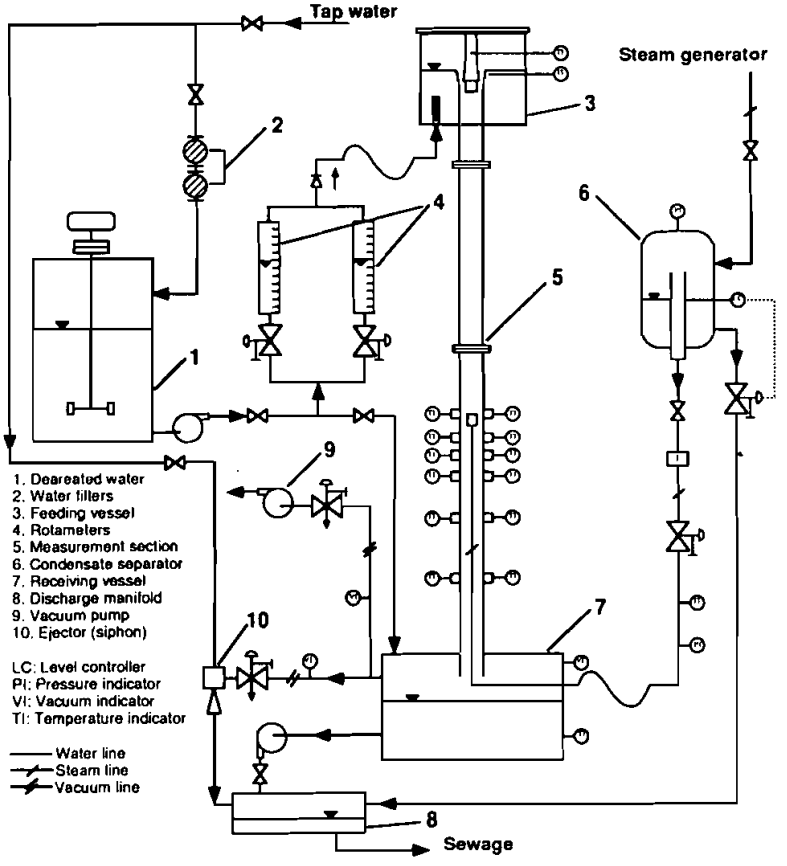

FIGURE 7 Experimental set-up.

pipe. The exact location of the tip of a thermocouple is a matter of concern. However, for the purpose of this study, measuring the temperature either close to the pipe surface or somewhat deeper into the film provides quite representative values of the average falling film temperature which is also verified by a separate set of experiments. It will be recalled that, for the flow rates employed in this study, turbulence and rolling down of waves tend to minimize all transverse temperature gradients in the film, in line with the preceding discussion in the Theory section. In this study only the last pair of thermocouples (at the downstream end of the pipe) was used to measure outlet liquid temperature. Thus the condensation length of the pipe, taken into account in the calculations, was 2.46 m. Sufficient external insulation was used to achieve practically adiabatic conditions.

Steam comes from the building supply at a pressure of 4 bar. It is passed through a conditioning setup involving two separators, a steam trap and a pressure regulator which reduces line pressure to only 1.5 atm so as to minimize the discharge velocity when entering the test pipe. This procedure provides a slightly superheated steam, relatively free of air ($< 10^{-3}$ mass fraction air in mixture). Excess steam is discharged to the atmosphere (in mixture with noncondensable air) through a vent located at the downstream receiving vessel. Experiments are made with air/steam mixtures saturated at 50° and 55°C.

Steam is released inside the pipe, at the center of the cross section, in the direction of the liquid flow. A specially designed feeding section made of a perforated teflon end-piece is used to spread the steam in the test tube, and minimize forced convection effects. The system is allowed to operate with steam, at a fixed liquid rate, for almost an hour to reach steady state. It is then observed that upon discharge to the test section, steam is mixed with air which enters the system from the top of the test pipe. There appears to be a net gaseous mixture movement downwards from the upper part of the pipe possibly through dragging by the interfacial shear, exerted by the fast moving liquid. On the other hand, natural convection tends to move steam-rich gaseous masses to the upper part of the pipe (above the steam entrance region), in the core of the tube. Visual observations suggest that the steam/air mixture moves with a finite velocity which, however, is under all circumstances small enough (well below 10 cm/s), compared with the liquid film velocity (of order 1 m/s). Thus, the gas phase may be considered effectively stagnant.

The steam entrance level is 1.77 m below the liquid feed. At that level the falling film flow is considered (e.g. Zabaras, 1985; Takahama and Kato, 1980) almost fully developed, facilitating the interpretation of local condensation measurements (Karapantsios, 1994). The average gas mixture temperature is obtained by integrating measurements over the entire pipe length. Higher temperatures are measured at the steam entrance region. However, gas/steam mixture temperature tends to be roughly uniform over most of the pipe length (above and below steam entrance) mainly due to the high percentage of noncondensables and the mixing effect resulting from the interplay between interfacial dragging and natural convection in the gas phase.

Filtered, deaerated tap water (stored in a large tank) is used in the test, flowing only once through the system. Flowrates from 36 to 490 g/s are employed. Copper-alumel thermocouples (T-type, 0.0508 cm diameter wire) are used for measurements with accuracy 0.1°C. The output temperatures are sampled at 3 Hz and processed by

a Thurlby 1905 miniprocessor equipped with an 8-bit A/D converter. Signal integration is performed for data acquisition periods of 3 to 10 minutes. Details of data collection and handling are given elsewhere, (Karapantsios, 1994). Repeatability checks are made for each set of conditions giving very satisfactory results.

A set of experiments is also conducted with a mild vacuum applied to the gas phase in the direction of the liquid flow as a means of exerting some shearing along the interface. For this purpose a vacuum manifold is employed consisting of a vacuum pump in parallel with a ejector (siphon). The vacuum manifold is permanently connected at the downstream receiving vessel, as shown in Figure 7. During preliminary tests, vacuum gauges were connected at all six plugs along the test section, to measure the vacumm variation along the tube. Under the relatively small vacumm level employed in all subsequent experiments, this variation was not very significant; i.e. at the tube bottom 0.1 bar underpressure was obtained while the topmost gauge (5 cm above steam release) showed 0.07 bar, both with and without liquid running inside the pipe. The vacuum pump was only used initially to reduce the air content inside the pipe, but for the main part of the vacuum experiments only the ejector was operated. The convective gas velocities created by the ejector could not be easily determined in the present tests. Nevertheless, to obtain first estimates of the influence of mild vacuum, results from these runs were directly compared with results from experiments without vacuum.

Special provisions are taken to eliminate vibrations caused by the pumps or the flow system. Flexible tubing and connections are used to reduce hydraulic pulsations, while special rubber pads and seals are employed to diminish mechanical vibrations.

RESULTS

For data reduction and calculations the following assumptions are made

- steam saturated throughout the pipe
- total gas pressure constant at 1 atm
- the gas/liquid interface is at saturation temperature T_S corresponding to steam partial pressure p_{vs}
- the liquid temperature profile is nearly flat at every section along the pipe, i.e. $T \cong T_{ave}$.

Thus the equality $T_{ave} = T_S$ emerges at each cross-section along the pipe. This assumed equality implies that the amount of latent heat released by the condensing steam is instantly absorbed by the flowing liquid, and consequently that the resistance to condensation resides entirely in the gas phase.

The overall condensation heat transfer coefficient, h, corresponding to the entire condensing surface (of length L) can be obtained as follows

$$h = \frac{\lambda}{T_g - T_f} \frac{\Delta Wc}{L} \tag{14}$$

with $T_f = (T_i + T_O)/2$ where T_i and T_O are liquid inlet and outlet temperatures, respectively, and $\Delta W_C/L$ is the condensation flux in $kg \cdot s^{-1} \cdot m^{-2}$. T_g is the average gas

mixture temperature. It could be argued that $\Delta T = T_g - T_f$, employed here for simplicity, may not be the appropriate choice to compute h but instead, one could integrate along the entire pipe by postulating a constant h throughout, using the corresponding logarithmic mean temperature difference, ΔT_{ln}. Sample calculations of h with $\Delta T_{ln} = (T_O - T_i)/\ln[(T_g - T_i)/T_g - T_O)]$ instead of $\Delta T = T_g - T_f$ for the conditions of our experiments did not show a change in the trend of data but only slightly in their values. The mean error in calculating h is estimated to be less than 15%.

A condensation efficiency is defined here

$$\Theta = \frac{T_O - T_i}{T_g - T_i} \tag{15}$$

which provides a measure of the water temperature increase as it relates to the overall available driving temperature difference. For the ideal case Θ must equal unity.

Figure 8 shows condensation efficiency plotted versus inlet liquid flow rate for all the experimental conditions examined. In all runs, a large amount of noncondensable air is used; i.e. $T_g = 50°C$ or $\sim 88\%$ air mole fraction and $T_g \doteq 55°C$ or $\sim 85\%$ mole fraction. As the liquid flow rate increases, the condensation efficiency decreases sharply at first. With further increase in W, the condensation efficiency still decreases but much more gradually. In both cases with vacuum applied, the condensation efficiency is larger compared with the cases without vacuum.

For the experiments with no vacuum, Θ is clearly higher for the gas bulk mixture with less air in it, $T_g = 55°C$. This holds true for all W. However, when a mild vacuum is

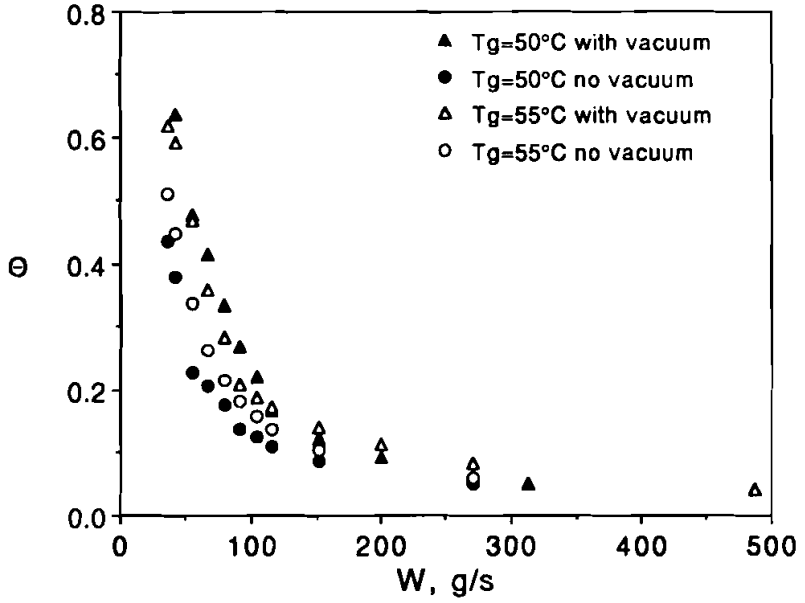

FIGURE 8 Condensation efficiency ($\Theta = T_O - T_i/T_g - T_i$) versus inlet liquid flow rate under various experimental conditions.

applied the influence of T_g appears to depend on liquid flow rates. In particular, at high W the efficiency Θ is higher for $T_g = 55°C$, while at low W somewhat higher Θ is obtained for $T_g = 50°C$. Whether this behavior represents a systematic trend should be investigated further over a broader range of conditions.

At very low liquid flow rates the efficiency is quite high, which means that good advantage is taken of the coolant capacity. For W larger than ~ 50 g/s the efficiency exhibits a drastic decrease. It is interesting to point out that for W smaller than 36 g/s (the minimum value employed in this work) it is impossible to maintain a continuous and uniform falling liquid layer; film rupture usually takes place, possibly due to surface tension effects. This was not observed in *isothermal* falling film experiments (Karapantsios *et al.*, 1989) for flow rates down to ~ 20 g/s. The film rupture phenomenon may in effect set an upper limit to condensation efficiency, at ~ 0.5 for this experimental system, which however may be raised by other means e.g. by applying vacuum on the gas phase.

In Figure 9 average heat transfer coefficients h ([14]), computed from the data, are plotted versus inlet liquid rate W. It is interesting, that h tends to decrease with increasing liquid rate. The same trend is obtained in a similar graph of condensation rate versus liquid rate. It must be also noted that data reported by Bontozoglou and Karabelas (1993) – their Figure 3 – for a direct contact condenser with structured packing, display a similar behavior for the upper part of the column where the amount of noncondesable gases is large. This is contrary to what one would observe in condensation of pure steam. An interpretation of this trend may be obtained by considering the large amount of noncondensables and the complex flow pattern that may develop in the gas phase by the interplay between the moving liquid interface and

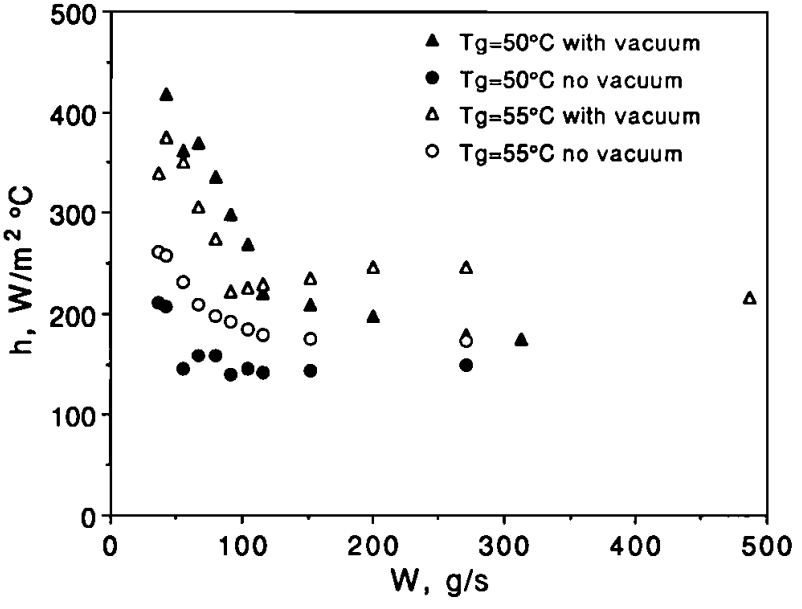

FIGURE 9 Condensation heat transfer coefficient h versus inlet liquid flow rate.

the adjacent gas layer, a situation of no particular significance when just pure steam is condensed. It is likely that the gas boundary layer b, greatly influenced by the gas flow distribution, is responsible for this behavior of the condensation rates. This point is further explored in a subsequent section.

An increase of the steam concentration in the gas phase results in higher condensation rates. The effect of vacuum is to cause a significant increase of condensation rates. This improved efficiency in the latter case is attributed to significant shear induced by forced convection. Shear creates agitation of the gas phase with the ultimate effect of reducing the thickness of the mass transfer boundary layer in the gas phase.

The favorable influence of vacuum has already been reported in the literature (e.g. Sideman and Maron, 1982) but only as a means to remove the noncondensables *locally* from the gas/liquid interphase. An increase of the overall heat transfer coefficient by even an order of magnitude due to this suction has been reported. Furthermore, all these studies deal with either horizontal channel flows (Pnueli and Iddan, 1971) or horizontal fan spray sheets (Tamir and Taitel, 1971) and not with vertical falling liquid films. Thus, no comparison can be made with the data of this study where mild vacuum was applied to the gas mixture.

Most literature work on the effect of noncondensables, as pointed out in the introduction, is restricted to relatively small ($\leqslant 10\%$) gas fractions, which nevertheless, cause tremendous reduction in heat transfer rates. Recent data by Ong'iro and Kanyua, (1990), for condensation over a horizontal solid wall, are also available with higher noncondensable mass fractions (up to 30%). Overall condensation heat transfer coefficients in the range 200 and 300 W/m^2 °C are obtained for 26% air concentration in the gas mixture, regardless of the inlet bulk gas temperature. Barry and Corradini, (1988), did direct-contact experiments in a horizontal channel with extremely high air-steam mass ratios, ($\sim 50\%$ to 94%). Turbulence and waviness of the liquid layers were present in their study. They reported overall heat transfer coefficients of about 200 to 600 W/m^2 °C. An important feature in their setup was the intensive forced convection on the gas side (gas velocities 5.5 and 6.5 m/s). In general the data from our study (e.g. Fig. 9) are in the same range of values with the results from both studies, even though different flow geometries and conditions are employed in the latter. This may be attributed to the large amount of noncondensables present in the gas phase, in which case the liquid hydrodynamics apparently plays a secondary role, the major resistance to condensation residing in the gas phase.

INFLUENCE OF WAVES ON THE APPARENT MASS TRANSFER BOUNDARY LAYER

In order to investigate the coupling between the liquid and the gas phase, the model equations are solved to obtain the apparent gas boundary layer thickness, b, for all the experiments of this study. This task is accomplished by requiring the average outlet liquid temperature T_O, calculated from the model to fit the experimentally measured one. Of course, this implies that all possible effects that may influence the condensation rate from the gas-phase side, (e.g. waviness, vapour flow due to interfacial drag) are combined to just one parameter, the gas boundary layer thickness. Figure 10 shows the

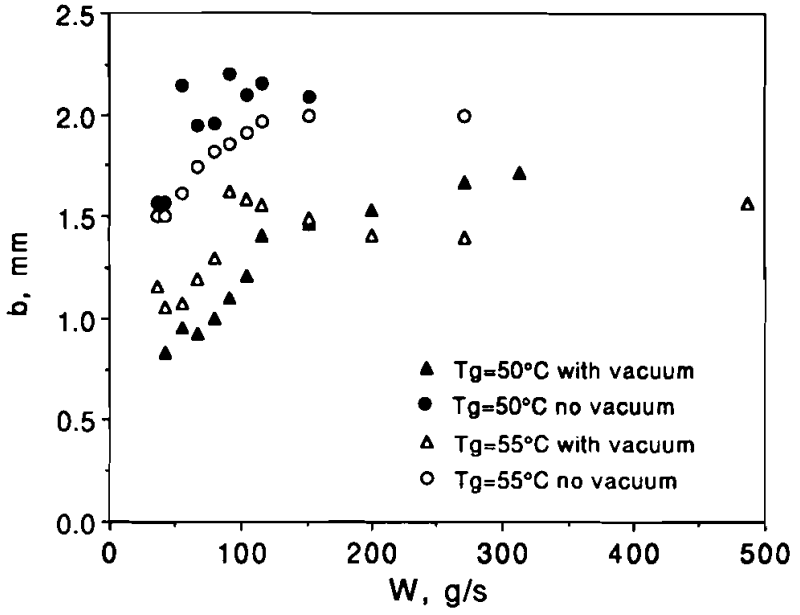

FIGURE 10 Apparent boundary layer b of noncondensables calculated from the present data.

gas phase boundary layer, b, plotted versus the inlet liquid flow rate, W, for all conditions examined in this study. The general trend for b is to gradually increase, finally levelling-off to an approximately constant value at higher W. As one might have expected, when no vacuum is applied the boundary layer is thicker. An increase up to 100% is observed between the cases with and without vacuum. Interestingly, the mass transfer boundary layer is of the same order magnitude as the liquid film thickness (Karapantsios *et al.*, 1989).

Comments similar to those presented in relation to Figure 9 may also be made for the variation of the apparent boundary layer thickness b (Fig. 10) at high noncondensable fractions. The literature is not helpful in this case since no relevant *condensation* data are available. Perhaps the most relevant work is the study of Akers *et al.* (1960) who examined condensation of ethanol and carbon tetrachloride on a *small* (3 inches long) vertical plate in the presence of nitrogen, helium and carbon dioxide. Their data are correlated with an empirical expression involving a Schmidt number Sc and a generalized Grashof number Gr. In effect, diffusion and free convection in the gas phase are assumed to be the only controlling mechanisms for the development of the gas boundary layer. The formula

$$\frac{L}{b} = 1.02(Gr\,Sc)^{0.373} \tag{16}$$

where $Gr = L^3 g \varrho^2 (\Delta\varrho/\varrho)/\mu^2$ and $Sc = \mu/\varrho D$, is recommended for vertical surfaces in the range $10^3 < Gr \cdot Sc < 10^7$ (laminar regime) and $0.3 < Sc < 3$. If this correlation is

applied to the conditions of the present tests, nearly constant thickness b is obtained i.e. $b = 0.329$ mm for $T_g = 50°C$ and $b = 0.319$ mm for $T_g = 55°C$, regardless of the liquid flow rate.

In the tests reported here the product $Gr \cdot Sc$ is of order 10^{10} and a turbulent rather than a laminar regime prevails. However, even a correlation for *turbulent* natural convection heat transfer (not available in literature for condensation) could not account for the experimentally observed increase of b with liquid flow rate. This disagreement indicates that natural convection and diffusion alone may not describe adequately phenomena that take place during condensation in systems like the present one. It seems that forced convection must be included to fully account for such a behavior.

Attention is now directed to the possibility that the statistical characteristics of the wavy falling film may have some bearing on the size of the apparent gas boundary layer b. The wavy falling film may, indeed, influence the neighboring gas phase, inhibiting or enhancing the growth of this diffusion layer. Statistical characterization of (isothermal) falling film hydrodynamics has already been carried out in this Laboratory (Karapantsios *et al.*, 1989; Karapantsios and Karabelas, 1990). In the latter study very significant local film thickness accelerations and decelerations (normal to the wall) are found to be associated with the roll wave motion. It is, thus, very likely that some complex momentum interchange may take place with the compressible gas phase, possibly inducing small scale local flow at the gas side.

Careful inspection of the data reported by Karapantsios *et al.* (1989), on the standard deviation s of the film thickness fluctuations (their Fig. 4), reveals that there may be a direct relationship between fluctuations of film thickness about its mean value and the gas boundary layer b. Figure 11 presents a typical film thickness trace where the mean (δ) and twice the standard deviation (2s) are also depicted. The film thickness trace as scaled in Figure 11 gives the false impression of the existence of narrow and steep roll waves. However, as Karapantsios and Karabelas (1990) reported, the true inclination of the wave front never exceeds about 20 degrees. It is evident that the value 2s can be considered as a representative measure of the average peak-to-trough distance of the film. Furthermore, this characteristic thickness (2s) may be linked to the mass transfer boundary layer, which implies a direct coupling of liquid film thickness fluctuations to the apparent gas diffusion boundary layer.

When vacuum is applied in the gas mixture, the resulting convective currents may tend to destroy the boundary layer above the waves, i.e. in the gaseous mass not sheltered in the troughs between waves. In that case, one may assume that b is reduced in size to a value roughly equal to 2s. Figure 12 illustrates this idea better, showing a striking similarity of the variation of gas boundary layer b determined from the condensation data, in the case of vacuum, and of the standard deviation (2s) of liquid film thickness fluctuations. This similarity and related arguments are only speculative since no other direct experimental evidence exists to relate the dffusion layer to film thickness fluctuations. Nevertheless, Figure 13 provides additional support to this idea. The computations of the overall heat transfer coefficient in this figure are based on (13) with 2s values substituted in place of the diffusion layer thickness b. The agreement between predictions and measurements is remarkable.

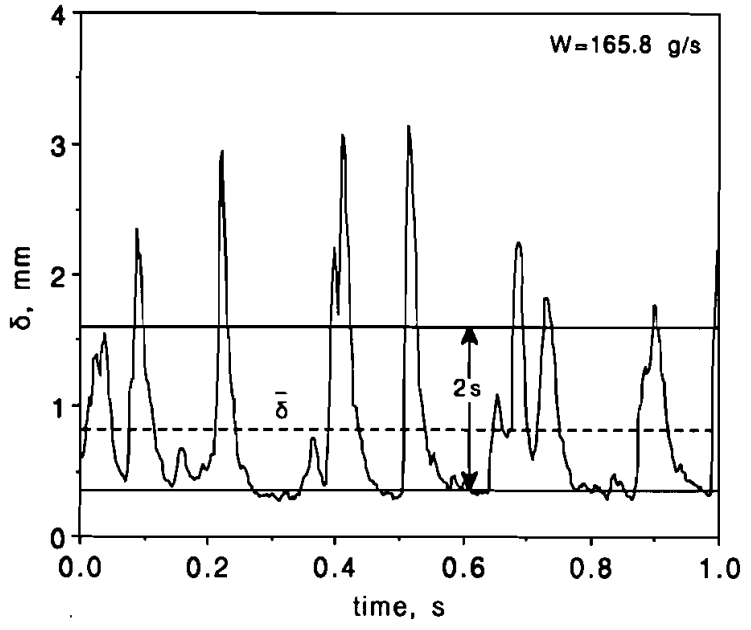

FIGURE 11 Typical film thickness time record with superposed two standard deviations (2s); δ is the mean film thickness.

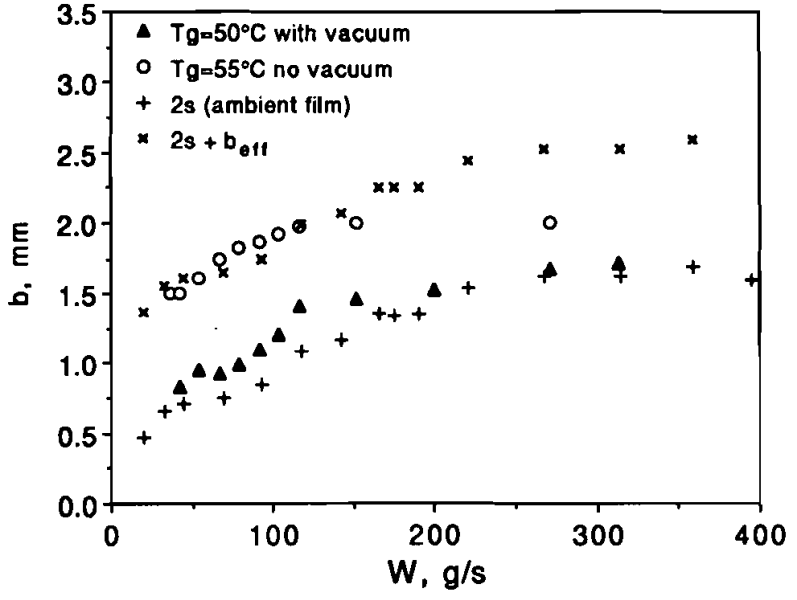

FIGURE 12 Experimentally determined apparent boundary layer of noncondensables, and comparison with available statistical information of film thickness fluctuations (Karapantsios *et al.*, 1989).

One may now go one step further. It is a natural extension of the above arguments to assume that, if no vacuum is applied, then the gaseous boundary layer is roughly the sum of a part attributed to gas sheltered inbetween waves and a part above the waves attributed to diffusion and convection effects. The latter part may be called effective diffusion layer (b_{eff}). A value $b_{eff} = 0.9$ mm is employed in Figure 12 (for comparison of data with predictions), using arguments not presented here due to space limitations. The good agreement, between the quantity ($2s + b_{eff}$) and the b values determined from the data, lends support to the hypothesis that the waves again influence the gas phase resistance in the case of no vacuum.

CONCLUDING REMARKS

A phenomenological description of a falling turbulent liquid film in contact with an effectively stagnant gas/vapor mixture is employed. It is shown that for the case considered here (large percentage of noncondensables) a significant simplification can be made in the mathematical description due to the fact that the main resistance to heat transfer resides in the gas phase. The liquid film itself does not seem to offer significant resistance to heat transfer. Consequently, a flat temperature profile across the liquid film provides a very satisfacory simplification. It is also shown theoretically that, for the high concentration of air employed in this study, the interfacial temperature varies almost linearly with condenser (pipe) length and that the contribution of sensible heat

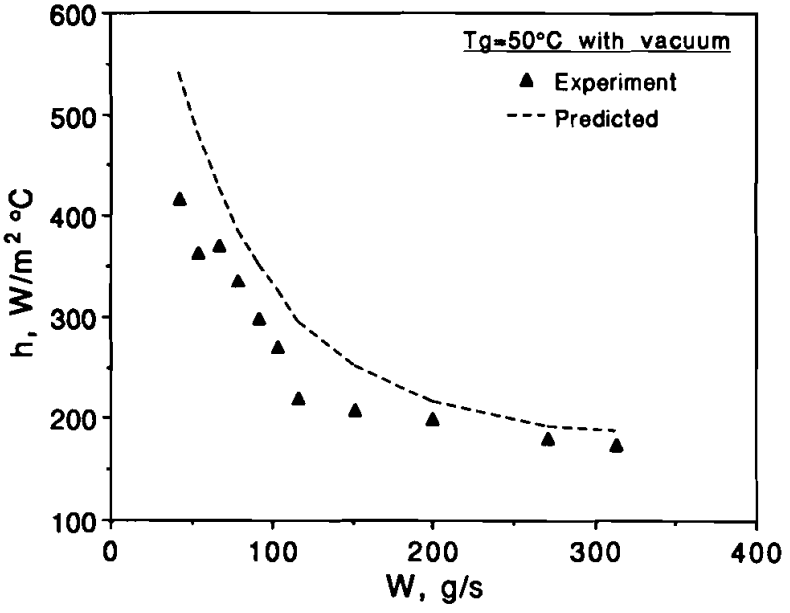

FIGURE 13 Condensation heat transfer coefficient versus liquid flow rate. Comparison between expermental data and predictions based on the assumption $b = 2s$ (standard deviation s from the data by Karapantsios *et al.*, 1989).

transfer is not very significant approaching only 10% of the overall heat transfer rate.

In this experimental effort, integral type of condensation data are collected to evaluate the overall performance of a relatively long test pipe which resembles in some ways a large part of a direct contact column condenser, under development in this Laboratory (Bontozoglou and Karabelas, 1993), for geothermal applications. The integral data reported here are helpful in improving our understanding and in preparing the ground for the development of design procedures.

The experimentally determined condensation heat transfer coefficients h display a rather unexpected trend; i.e. a decreasing h, with increasing liquid flow rate, which tends to reach an asymptotic value. A similar behaviour is also obtained in the aforementioned direct contact condensation column. This interesting trend may be attributed to the thickening of an effective boundary layer rich in noncondensables. This thickening may be aided by local currents at the interface on the gas mixture side (possibly induced by the wavy liquid motion) that may not be effectively counterbalanced by lateral diffusion.

Tests to explore the influence of a mild vacuum on the condensation rates show that it can significantly improve such rates. In the data reported here an increase of condensation rate by as much as 100% is noted, and it is ascribed to the thinning of the gas diffusion layer (at the interface) possibly caused by small convective currents.

The gas phase may be regarded as quasi-stagnant insofar as its bulk velocity is small relative to the liquid surface velocity. However, the wavy liquid surface may induce local convective motions in the gas phase or may interact with it otherwise modifying the gas mixture concentration gradients. Such considerations are irrelevant in the case of pure steam condensation. Along these lines, an interesting observation is made by comparing the independently measured standard deviation (s) of liquid thickness fluctuations to the gas diffusion layer thickness (b) determined from the condensation experiments. The quantity $2s$ appears to be (at least qualitatively) quite representative of wave effects on the gas side resistance to heat transfer. Furthermore, for vacuum applied, using $2s$ instead of b the theoretical predictions of condensation heat transfer coefficient h are in good agreement with measured h values. This observation suggests that the wavy liquid layer strongly influences the diffusion layer, possibly through a complex momentum exchange type of mechanism. It will be pointed out that the very significant (Eulerian) accelerations and decelerations of the liquid interface normal to the wall, reported by Karapantsios and Karabelas (1990), may be at the heart of such a mechanism.

ACKNOWLEDGEMENT

This work has been supported in part by the General Secretariat for Research and Technology of Greece and by the Commission of European Communities (under programme VALOREN). Helpful discussions with Dr. V. Bontozoglou are greatly appreciated. The authors also thank Mr. G. P. Chatzimavroudis for his help in data collection.

NOMENCLATURE

A, B	Constants,/
b	Apparent mass boundary layer at the gas side, m
b'	Apparent thermal boundary layer at the gas side, m
c_1, c_2	Constants,/
c_p	Specific heat, $J\,kg^{-1}\,°K^{-1}$
D	Tube diameter, m
D_g	Binary mass diffusivity coefficient, $m^2\,s^{-1}$
Fo	Liquid Fourier number $(\alpha L/u\delta^2)$,/
g	Gravity acceleration, $m\,s^{-1}$
Gr	Gas Grashof number $(L^3 g\varrho\Delta\varrho/\mu^2)$,/
h	Condensation heat transfer coefficient, $W\,m^{-2}\,°K^{-1}$
h_g	Sensible heat transfer coeffiicient on the gas side (k_g/b'), $W\,m^{-2}\,°K^{-1}$
k	Thermal conductivity, $W m^{-1}\,°K^{-1}$
K_g	Mass transfer coefficient on the gas side (D_g/b), $m\,s^{-1}$
L	Distance between measuring stations, m
Nu	Liquid Nusselt number $(h\delta/k)$, /
p	Partial pressure, /
p_{am}	Log mean partial presssure of noncondensable air $(p_{as} - p_{ag})/\ln(p_{as}/p_{ag})$, /
q	Local heat flux, $W\,m^{-2}$
s	Standard deviation, m
Sc	Gas Schmidt number, $(\mu/\varrho D_g)$, /
T	Temperature, °K
t	Time, s
y	Distance in the radial direction, m
u	Local velocity component in the flow direction, $m\,s^{-1}$
U_{ave}	Average streamwise velocity, $m\,s^{-1}$
W	Liquid flow rate, $kg\,s^{-1}$
x	Distance in the axial direction, m

Greek symbols

α	Molecular thermal diffusiviy, $m^2\,s^{-1}$
α_e	Effective thermal diffusivity, $m^2\,s^{-1}$
Γ	Mass flow rate per unit width, $kg\,m^{-1}\,s^{-1}$
δ	Film thickness, m
Θ	Dimensionless temperature, /
λ	Latent heat, $J\,kg^{-1}$
μ	Dynamic viscocity, $kg\,m^{-1}\,s^{-1}$
ν	Kinematic viscocity, $m^2\,s^{-1}$
ϱ	Density, $kg\,m^{-3}$

Subscripts

a	Air
ave	Average

eff	Effective
g	Bulk
i	Inlet
o	Outlet
s	Surface
v	Vapour
w	Wall

REFERENCES

Akers, W. W., Davis, S. S., and Crawford. J. E., Condensation of a Vapor in the Presence of a Non-Condensing Gas, *Chem. Eng. Prog. Symp. Series*, **56**, 139–144 (1960).

Bankoff, S. G., and Kim, H. J., Local Condensation Rates in Nearly Horizontal Stratified Countercurrent Flow of Steam and Cold Water, *A.I.Ch.E. Symp. Series*, **79**, 209–223 (1983).

Barry, J. J., and Corradini, M. L., Film Condensation in the Presence of Interfacial Waves, *ASME Proceedings of the 1988 National Heat Transfer Conference*, Houston, TX, 523–529 (1988).

Barry, J. J., Effects of Interfacial Structure on Film Condensation, PhD Thesis, University of Wisconsin-Madison (1987)

Bontozoglou, V., and Karabelas, A., An Experimental Study of Direct Contact Steam Condensers an Noncondensable Gas Separators, *Energy Efficiency in Process Technology* edited by P. A. Pilavachi, pp. 465–474, Elsevier, London, (1993).

Celata, G. P., Cumo, M., D'Annibale, D., Farello, G. E., and Focardi, G., A Theoretical and Experimental Study of Direct-Contact Condensation on Water in Turbulent Flow, *Experim. Heat Transfer*, **2**, 129–148 (1989).

Celata, G. P., Direct Contact Condensation of Steam on Subcooled Water, *Phase-Interface Phenomena in Multiphase Flow* edited by G. F. Hewitt, F. Mayinger and J. R. Riznic, Hemisphere, New York (1991).

Collier, J. G., *Convection Boiling and Condensation*, McGraw-Hill, London (1972).

Fair, J. R., and Bravo, J. L., Distillation Columns Containing Structured Packing, *Chem. Eng. Prog.*, **86**(1), 19–29 (1990).

Finkelstein, Y., and Tamir, A., Interfacial Heat Transfer Coefficients of Various Vapors in Direct Contact Condensation, *The Chem. Engin. J.*, **12**, 199–209 (1976).

Jacobs, H. R., Condensation on Immiscible Falling Films, *ASME paper No. 80-HT-110*, Orlando, FL (July 1980).

Jacobs, H. R., Direct Contact Condensation (pp. 223–236) in *Direct-Contact Heat Transfer* (F. Kreith and R. F. Boehm, Editors), Hemisphere, New York (1988).

Karapantsios, T. D., and Karabelas, A. J., Surface Characteristics of Roll Waves on Free Falling Films, *Int. J. Multiphase Flow*, **16**, 835–852 (1990).

Karapantsios, T. D., Flow of a Thin Liquid Film in a Vertical Pipe. Direct-contact condensation phenomena, Ph. D. Thesis (in Greek), Univ. of Thessaloniki (1994).

Karapantsios, T. D., Paras, S. V., and Karabelas, A. J., Statistical Characteristics of Free Falling Films at High Reynolds Numbers, *Int. J. Multiphase Flow*, **15**, 1–21 (1989).

Kim, H. J., Lee, S. C., and Bankoff, S. G., Heat Transfer and Interfacial Drag in Countercurrent Steam-Water Stratified Flow, *Int. J. Multiphase Flow*, **11**, 593–606 (1985).

Kreith, F., and Boehm, R. F., (Editors), *Direct-contact heat transfer*, Hemisphere, New York, (1988).

Minkowycz, W. J., and Sparrow, E. M., Condensation Heat Transfer in the Presence of Noncondensables, Interfacial Resistance, Superheating, Variable Properties and Diffusion, *Int. J. Heat Mass Transfer*, **9**, 1125–1144 (1966).

Mudawar, I., and El-Masri, M. A., Momentum and Heat Transfer Across Freely-Falling Turbulent Liquid Films, *Int. J. Multiphase Flow*, **12**, 771–790 (1986).

Ong'iro, A. O., and Kanyua, J. F., Tube Side Condensation of Steam in the Presence of a Non-condensable Gas, *Geothermal Resources Council TRANSACTIONS*, **14**, 337–341 (1990).

Pnueli, D., and Iddan, G., Heat and Mass Transfer in Condensation on the Surface of a Moving Fluid in the Presence of Non-condensable Gas with Suction at the Interface, *Desalination*, **9**, 285–294 (1971).

Rao, V. D., and Sarma, P. K., Condensation Heat Transfer on Laminar Falling Film, *ASME J. of Heat Transfer*, **106**, 518–523 (1984).

Sideman, D., and Moalem-Maron, D., Direct Contact Condensation, *Advances in Heat Transfer*, **15**, 227–281 (1982).

Takahama, H., and Kato, S., Longitudinal Flow Characteristics of Vertically Falling Liquid Films Without Concurrent Gas Flow, *Int. J. Multiphase Flow*, **6**, 203–215 (1980).

Tamir, A., and Rachmilev, I., Direct Contact Condensation of an Immiscible Vapor on a Thin Film of Water, *Int. J. Heat Mass Transfer*, **17**, 1241–1251 (1974).

Tamir, A., and Taitel, Y., Improving Condensation Rate by Interfacial Suction and Forced Convection in the Presence of Non-condesables, *Isr. J. Technol.*, **9**, 69–81 (1971).

Ueda, H., Moller, R., Komori, S. and Mizushina, T., Eddy diffusivity Near the Free Surface of Open Channel Flow, *Int. J. Heat Mass Transfer*, **20**, 1127–1136 (1977).

VDI-Wärmeatlas, Berechnungsblätter für den Wärmeübergang, 2. Auflage, VDI-Verlag GmbH, Dusseldorf, (1974).

Zabaras, G. J., Studies of Vertical Annular Gas-Liquid Flows, Ph.D. Thesis in Chem. Engng., University of Houston (1985).

APPENDIX

A quick preliminary assessment of the influence of various parameters on the heat transfer process, depicted in Figure 1, can be made by using the results of the following analysis. To obtain closed form solutions, constant velocity u and thermal diffusivity $\alpha = k/\varrho c_p$ are assumed for the liquid film. Thus the energy equation for the thermal field inside the film is written as

$$u\frac{\partial T}{\partial x} = \alpha\frac{\partial^2 T}{\partial y^2} \qquad [A1]$$

with general boundary conditions

$$\text{at the entrance,} \quad x = 0 \quad T = T_i \qquad [A2]$$

$$\text{at the interface,} \quad y = 0 \quad -k\frac{\partial T}{\partial y} = h_s(T_s - T) \qquad [A3]$$

$$\text{at the solid wall,} \quad y = \delta \quad -k\frac{\partial T}{\partial y} = h_w(T_w - T) \qquad [A4]$$

Here the subscripts s and w designate conditions at the gas/liquid interface and at the solid wall, respectively.

The following dimensionless variables and parameters are introduced

$$\Theta = \frac{T - T_i}{T_s - T_i}, \quad x = \frac{x}{L}, \quad y = \frac{y}{\delta}$$

$$f \equiv Fo = \frac{\alpha L}{u\delta^2}, \quad A \equiv Nu_s = \frac{h_s\delta}{k}, \quad B \equiv Nu_w = \frac{h_w\delta}{k}$$

where L is the length of the condensing section Fo designates a Fourier number, which may also be viewed as the inverse of a modified Graetz number (ratio of convective over conductive transfer). Equation [A1] with B.C.'s [A2]–[A4] become

$$\frac{\partial\Theta}{\partial x} = f\frac{\partial^2\Theta}{\partial y^2} \qquad [A5]$$

$$x = 0 \quad \Theta = 0 \qquad [A6]$$

$$y=0 \quad \frac{\partial\Theta}{\partial y}=-A(1-\Theta) \tag{A7}$$

$$y=1 \quad \frac{\partial\Theta}{\partial y}=-B(\Theta-\Theta_w) \tag{A8}$$

The solution of differential Equation [A5] is given by

$$\Theta=c_1 y+c_2-\sum_{n=1}^{\infty}\frac{a_n'}{a_n''}\left[\sin(\lambda_n y)+\frac{\lambda_n}{A}\cos(\lambda_n y)\right]\exp(-\lambda_n^2 fx) \tag{A9}$$

where

$$c_1=\frac{AB(\Theta_w-1)}{A+B+AB}, \quad c_2=\frac{A+AB+B\Theta_w}{A+B+AB} \tag{A10}$$

$$a_n'=c_1\left(\frac{\sin(\lambda_n)}{\lambda_n^2}-\frac{\cos(\lambda_n)}{\lambda_n}\right)+c_2\left(\frac{1}{\lambda_n}-\frac{\cos(\lambda_n)}{\lambda_n}\right)+\frac{c_1}{A}\left(\sin(\lambda_n)+\frac{\cos(\lambda_n)}{\lambda_n}-\frac{1}{\lambda_n}\right)+\frac{c_2}{A}\sin(\lambda_n) \tag{A11}$$

$$a_n''=\frac{1}{2}-\frac{\sin(2\lambda_n)}{4\lambda_n}+\frac{\sin^2(\lambda_n)}{A}+\frac{\lambda_n^2}{A^2}\left(\frac{1}{2}+\frac{\sin(2\lambda_n)}{4\lambda_n}\right) \tag{A12}$$

with λ_n obtained from

$$\frac{\lambda_n\tan(\lambda_n)}{A}=\frac{1+B/A}{1-AB} \tag{A13}$$

One may now examine the temperature profile within the liquid film under various conditions; e.g. large or small convection (using $f\equiv Fo$), adiabatic ($B=Nu_w=0$) or nonadiabatic ($B\neq 0$) solid wall, considering a finite ($A=Nu_s\neq 0$) or negligible resistance at the gas/liquid interface. For a given physical situation, it is relatively easy to estimate the magnitude of the dimensionless groups Fo and Nu_w, while (as discussed in this paper) order of magnitude differences may be observed in the range of variation of h_S (and of $A=Nu_S$) even within the same equipment. One should, therefore, pay special attention to the influence of A on the heat transfer process.

For the system examined in this work, adiabatic conditions are assumed for the solid wall ($B=0$), and a finite resistance ($A\neq 0$) at the vapor side which actually controls the condensation process.

For such conditions the solution to [A5] is of the form

$$\Theta=1-\sum_{n=1}^{\infty}\frac{2\sin(\lambda_n)}{\lambda_n+\sin(\lambda_n)\cos(\lambda_n)}\cos(\lambda_n(1-y))\exp(-\lambda_n^2 fx) \tag{A14}$$

with values of λ_n computed from

$$\lambda_n\tan(\lambda_n)=A \tag{A15}$$

If in particular, $f\cdot x>0.5$ (which holds just after a few centimeters in the direction of flow for our system) and $A<1.0$ one may keep only the first term of the series in [A14].

Then, λ_1 is given by the perturbation solution of [A15], that is

$$\lambda_1 = A^{0.5}\left(1 - \frac{1}{6}A + \frac{11}{360}A^2\right) \qquad [A16]$$

Further, if $A < 0.1$, Θ is given by

$$\Theta = 1 - \left(1 - \frac{A}{2}y\right)\exp(-Afx) \qquad [A17]$$

and finally, if $A \ll 1$, e.g. $O(10^{-2})$, then the solution for the dimensionless temperature Θ becomes independent of y

$$\Theta = 1 - \exp(-Afx) \qquad [A18]$$

Equation [A18], shows that for such a set of parameters the temperature profile across the liquid film is flat (independent of y) which in turn indicates that the resistance to heat transfer resides entirely in the gas phase.

It is pointed out that in the steam/water system studied here, both f and A are usually of order 1.0. In the latter case, [A18] suggests that the deviation from the flat temperature profile is at most 5%. The simplified appproach given in this Appendix is obviously useful for preliminary estimates.